The Rotational Axis Approach for Resolving the Kinematic Redundancy of the Human Arm in Reaching Movements

Zhi Li, Jay Ryan Roldan, Dejan Milutinović and Jacob Rosen

***Abstract*— The human arm is kinematically redundant with respect to reaching tasks in a 3 dimensional (3D) workspace. Research on reaching movements of the healthy human arm reveals the control strategy of the human motor system, which can be further applied to the upper limb exoskeletons used for stroke rehabilitation. Experiments performed on ten healthy subjects have shown that when reaching from one point to another, the human arm rotates around an axis going through the shoulder. The proposed redundancy resolution based on the direction of the axis can predict the arm posture with a higher accuracy comparing to a redundancy resolution that maximizes the motion efficiency. It is also shown that for reaching movements in the comfortable arm motion range, the directions of the axis are constrained by a linear model.**

I. Introduction

The synergy of the human arm and upper limb exoskeletons benefits many medical applications such as stroke rehabilitation. An upper limb exoskeleton that is compatible with the human arm possesses seven degrees of freedom (DOFs) and is therefore kinematically redundant with respect to reaching and grasping tasks defined by six DOFs. Here we study reaching movements of the healthy human arm to reveal a control strategy of the human motor system, for its application to the control of upper limb exoskeletons (Fig. 1).

Fig. 1. The upper limb exoskeleton with seven DOFs, supporting 99% of the range of motion required to preform daily activities.

When solving an inverse kinematics or dynamics problem for manipulation tasks, redundant degrees of freedom can be used to achieve secondary goals such as to satisfy certain task constraints or to improve task performances. Task-based redundancy resolutions control the extra DOF by integrating the task-dependent constraints into an augmented Jacobian matrix [1], [2]. The performance-based redundancy resolutions may optimized the manipulability [3], [4], [5], [6], energy consumption [7], [8], smoothness of movement [9], [10], [11], [12], task accuracy [13] and control complexity [14].

Zhi Li (zhil@soe.ucsc.edu), Jay Ryan Roldan (juroldan@ucsc.edu), and Jacob Rosen (rosen@soe.ucsc.edu) are with the Department of Computer Engineering, Dejan Milutinović (dejan@soe.ucsc.edu) is with the Department of Applied Mathematics & Statistics, University of California, Santa Cruz, CA 95064, USA

Bionics Lab URL: http://bionics.soe.ucsc.edu/

II. Kinematic Model of the Human Arm

A. Representation of the Redundant Degree of Freedom

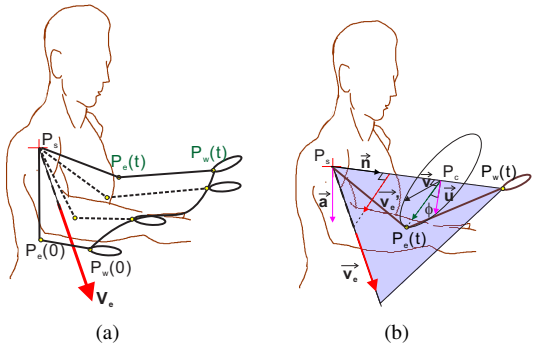

Fig. 2. Hypothesis: when reaching from one target to another in free space, the arm plane defined by shoulder (P_s), elbow (P_e) and wrist position (P_w) rotates about a virtual rotational axis.

The kinematics of the human arm in reaching movements involves four DOFs: three at the shoulder joint and one at the elbow joint. Given a fixed wrist position in a 3D workspace, elbow can move around an axis that connects the shoulder and the wrist due to the kinematic redundancy. The redundant DOF can be represented by a swivel angle ϕ (see Fig. 2(b)). The direction of the axis that the elbow pivots about (denoted by $\boldsymbol{n}$) is defined as:

$$\vec{n} = \frac{P_w - P_s}{||P_w - P_s||} \tag{1}$$

The plane orthogonal to $\vec{n}$ can be determined given the position of P_e. P_c is the intersection point of the orthogonal plane with the vector $P_w - P_s$. $P_e \vec{-} P_c$ is the projection of the upper arm ($P_e \vec{-} P_s$) on the orthogonal plane. $\vec{u}$ is the projection of a normalized reference vector $\vec{a}$ onto the plane orthogonal, which can be calculated as:

$$\vec{u} = \frac{\vec{a} - (\vec{a} \cdot \vec{n})\vec{n}}{||\vec{a} - (\vec{a} \cdot \vec{n})\vec{n}||} \tag{2}$$

The swivel angle ϕ, represents the arm posture, can be defined by the angle between the vector $P_e \vec{-} P_c$ and $\vec{u}$. The

reference vector $\vec{a}$ is suggested to be $[0, 0, -1]^T$ such that the swivel angle $\phi = 0°$ when the elbow is at its lowest possible point [**?**].

B. Redundancy Resolution: the rotational axis method

Our proposed redundancy resolution focuses on reaching movements between two points in a 3D workspace. It is based on the observation that during the reaching movement, the arm plane (i.e., the plane formed by the positions of the shoulder, the elbow and the wrist) rotates about an axis that going through the shoulder position. Given the direction of the axis, the position of the elbow always falls on the plane formed by the rotational axis and the wrist position.

In Fig. 2(b), $\vec{v_e'}$ is the vector component of the rotational axis direction $\vec{v_e}$ perpendicular to $\vec{n}$, i.e, the vector rejection of $\vec{v_e}$ from $\vec{n}$. Given that $\vec{v_e'}$ is parallel with the vector $P_e - P_c$, the swivel angle can be estimated as:

$$\phi = arctan2(\vec{n} \cdot (\vec{v_e'} \times \vec{u}), \vec{v_e'} \cdot \vec{u}) \quad (3)$$

C. The Equilibrium Posture of the Human Arm

While it is possible that the rotational axis varies depending on the region in which the human arm performs a task, a good candidate for the rotational axis is the direction of the equilibrium vector. It is known that when the human arm rest in the equilibrium posture, the periarticular muscles are in the position of minimal muscle actuation. In the equilibrium posture, a human arm with fractures of the shoulder and of the upper arm can be rested in the position of immobilization for proper recovery. The arm postures that are derived from the equilibrium arm posture may be naturally preferred for redundancy resolution.

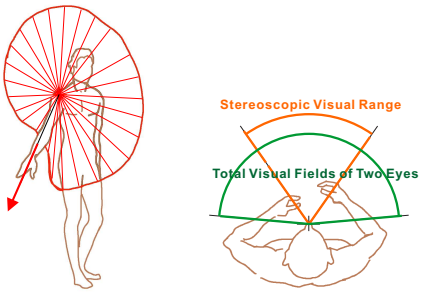

(a) (b)

Fig. 3. (a) Equilibrium posture directs the arm to its position of equilibrium of the periarticular muscles, and (b) brings the working hands in the range of stereoscopic visual control.

In Fig. 3(a), the red arrow pointing from the center of the shoulder denotes the axis the circumduction cone, which corresponds to the motion range of a healthy human arm. When the upper arm is aligned in the direction of the red arrow, the human arm is in the position of equilibrium of the periarticular muscles. As shown in Fig. 3(b), the equilibrium arm posture naturally directs the upper arm so that the working hands lie in the sector of preferential accessibility and stay in the visual control [15].

Fig. 3(b) illustrates that for the equilibrium posture the range of accessible points in the task space overlaps with the stereoscopic visual range. This coincidence is likely a result of interactions between morphology (e.g., structures and arrangements of joint and muscles), actuation (e.g., the way that muscles actuate joints) and sensory feedback (e.g., visual feedback) in evolutionary development. It strongly affects the control strategies of human motor system, e.g., the way that human arm moves given its kinematic redundancy.

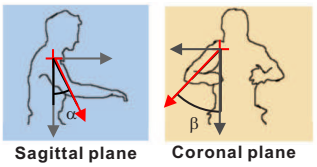

Fig. 4. The direction of the rotational axis can be specified by the flexion angle (α) and abduction angle (β). The direction of equilibrium posture of the upper arm is a possible candidate for the direction of the rotational axis.

The neutral body posture (NBP), including the direction of the equilibrium vector for the upper arm, has been experimentally investigated by NASA [16]. In the microgravity condition, the estimated shoulder flexion is about $36°$ and the shoulder abduction is about $50°$. As shown in Fig. 4, the angles of flexion α and abduction β are measured from the projection of the equilibrium direction on the sagittal plane and coronal plane, respectively. Studies in Skylab collected static measurements from 12 subjects. Due to a small sample size and possible imprecision, further investigation took the general anthropometric body measurements from all six STS-57 crew members. The results showed that the NBP differed for different subjects within a wide range.

III. Experiment: Posture of a Healthy Human Arm in Reaching Movements

This section conducts experiment and confirms that when the human arm reach from one target to another, the plane of the arm rotates about an axis. The direction of the rotational axis varies for reaching movements between different targets, however it is constrained to a surface for the reaching movements within a comfortable motion range, where the subjects do not need to stretch their arms to the joint limits to reach the targets. The rotational axis will deviate from the constraining surface due to the blocking effect of the torso, when the reaching movements are close to the boundary of the arm motion range.

A. Experiment Protocol

Ten healthy subjects (six males and four females) are instructed to conduct reaching movements with their right arms to each of the eight targets specified in the spherical workspace (Fig. 6). Each subject performs eight reaching movement sessions. Reaching movements of the same

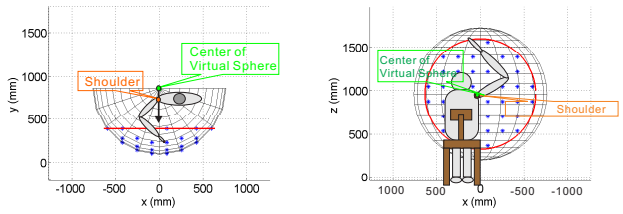

(a) Top View. (b) Front View

Fig. 5. The spherical workspace for experiments of the reaching movements: (a) the top view and (b) the front view.

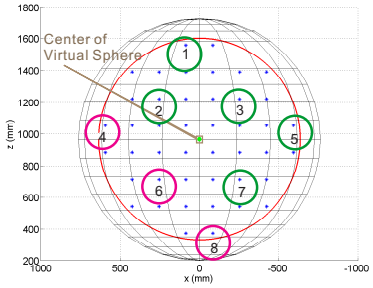

Fig. 6. Targets in the reaching movement experiment. For the right arm, target 1, 2, 3, 5, 7 (in green circles) are within the comfortable arm motion range while target 4, 6, and 8 (in magenta circles) are close to the motion range boundary

session start from one of the remaining seven targets. A complete session consists of five repetitions of seven different movements. The total number of trials for each subject is $8 \times 7 \times 5 = 280$.

During the experiment, a subject sits in a chair with a straight back support. The chair is placed in the way that the subject can point at the targets with comfort and with his/her naturally flexed elbow. The height of the workspace center is adjustable and it is always aligned with the right shoulder of the subject. The right arm is free for reaching movements, but the body of the subject is bounded to the chair back, which minimizes the shoulder displacement. During the reaching movements, subjects keep the pointing fingers in line with the forearm to minimize wrist flexion.

Subjects are asked to point with the index finger tip at their comfortable paces. At the beginning of each trial, the subject is informed of the targets that the trajectory starts with and ends at, i.e., the start target and end target. After receiving a "start" command, the subject moves his/her index finger from the start target to the end target.

A motion capture system records a single file for each trial. The recording starts from the time when the subject points the index finger to the start target and ends after the index finger tip becomes steady at the end target. To avoid the effect of fatigue, subjects take a rest after completing each session.

B. Experiment Results

Fig. 7 shows the statistics of the prediction error for all the valid trails (2680 out of 2800) conducted by ten subjects.

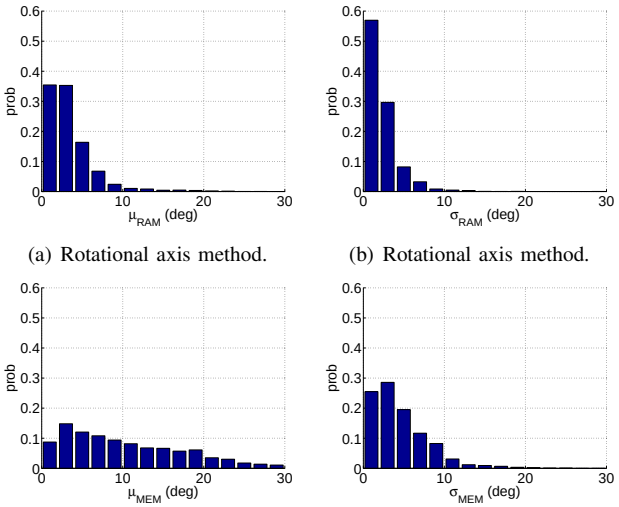

(a) Rotational axis method. (b) Rotational axis method.

(c) Motion efficiency method. (d) Motion efficiency method.

Fig. 7. Performance comparison of two swivel angle estimation methods by the distributions of the mean and standard deviation of estimation error.

The swivel angle prediction based on the rotational axis method (RAM) and by the motion efficiency method (MEM) proposed by [6] are calculated for comparison. The mean and standard deviations of the prediction error are denoted by μ_{RAM}, μ_{MEM}, and σ_{RAM}, σ_{MEM} respectively.

Based on RAM, 79.59% of the trials have both $\mu_{RAM} \leq 5^\circ$ and $\sigma_{RAM} \leq 5^\circ$. 3.92% trials have either $\mu_{RAM} \geq 10^\circ$ or $\sigma_{RAM} \geq 10^\circ$. Therefore, with respect to the mean value and the variance, RAM predictions outperform MEM predictions (see Fig. 7). The direction of the axis can be estimated for each trial based on the measured shoulder, elbow and wrist position.

Fig. 8 shows the estimated direction of the rotational axis in each of the movements. The vector of the rotational axis always points from the shoulder position and its direction is measured by the abduction and flexion angles. The yellow dots represent the estimated directions of the rotational axis for each trial. Some of the yellow dots are highlighted by either green circles or magenta circles, corresponding to the movements between target 1, 2, 3, 5 and 7, and the movements between target 4, 6 and 8, respectively. Note that for the right arm, target 1, 2, 3, 5, 7 are within the comfortable arm motion range while target 4, 6, and 8 are close to the motion range boundary.

A linear data fit is performed to summarize the relation between the abduction and flexion of a rotational axis (see Fig. 8). The regression method iteratively re-weights least squares with the bi-square weighting function so that the effect of outliers can be reduced [17]. The line describes a surface constraining the rotational axis when the right arm moves within the comfortable motion range. For the movements close to the boundary of arm motion range (i.e., between target 4, 6 and 8), the estimated directions of the rotational axis strongly deviate from the line. The blue dot in Fig. 8 represents the direction of the equilibrium vector

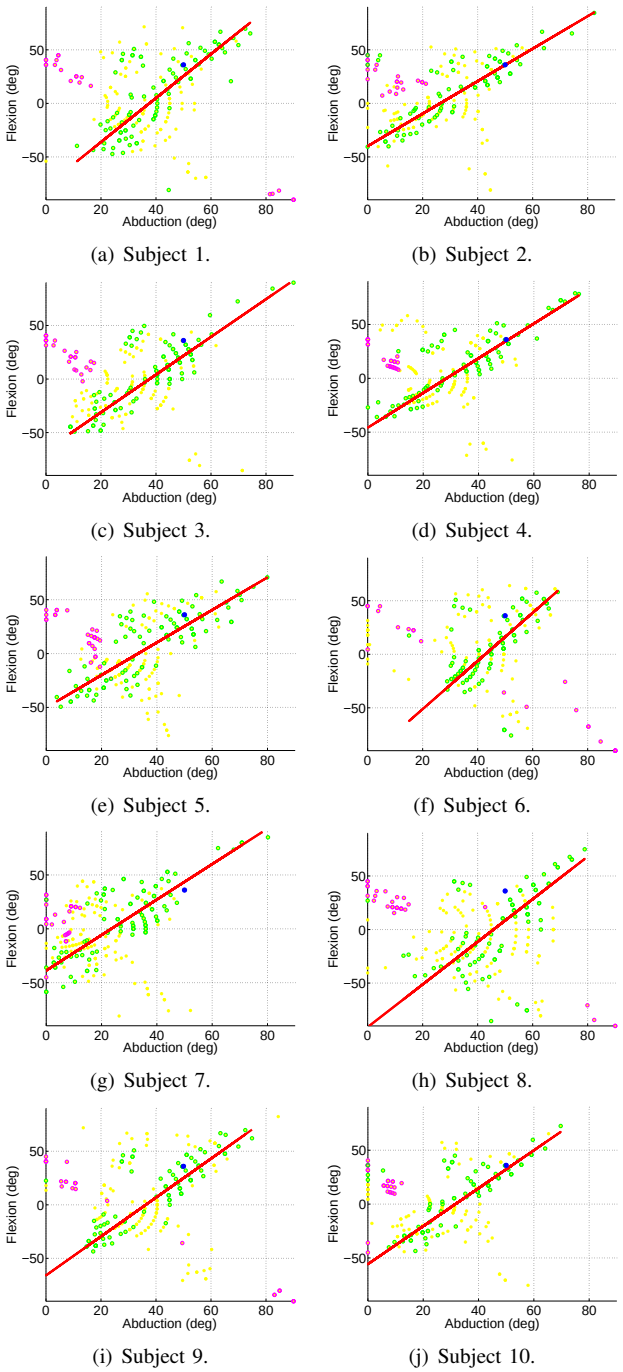

Fig. 8. The directions of the rotational axis are estimated for each valid trial. A linear regression model describes the surface that constrains the axis direction when the right arm moves in its comfortable motion range.

measured in microgravity condition by NASA [16]. It is close to our linear relation and therefore is one possible directions of the rotational axis when the arm moves between the targets in the comfortable motion range.

IV. Conclusion

In this paper we studied reaching movements of the human arm in a 3D workspace. Our reaching movement experiment results show that the arm plane (defined by the shoulder, elbow and wrist position) rotates about an axis going through the shoulder position. For reaching movements in the comfortable motion range, the rotational axis directions are constrained to a surface, which can be parameterized by a linear model. For reaching movements close to the boundary of the motion range, the directions deviate from the surface most likely due to the blocking effect of the torso.

The existence of the rotational axis and the constraining surface may reveal a relationship between path planning and redundancy resolution from another perspective. It is possible that knowing the start and end points, human motor control system influences a preferred direction of the axis so that by rotating about the axis, the human arm can easily bring the hand from the start point to its destination. Further research will be conducted to find out how to specify the direction of the rotational axis on the constraining surface, given the start and end points in the workspace, and to integrate the path planning and redundancy resolution in a general algorithm.

References

[1] L. Sciavicco, "A dynamic solution to the inverse kinematic problem for redundant manipulators," in *ICRA 1987*, vol. 4, pp. 1081–1087.

[2] ——, "A solution algorithm to the inverse kinematic problem for redundant manipulators," *IEEE Trans. Robot. Automat.*, vol. 4, no. 4, pp. 403–410, 1988.

[3] H. Asada and J. Granito, "Kinematic and static characterization of wrist joints and their optimal design," in *ICRA 1985*, St. Louis, Missouri, Mar. 1985, pp. 244–250.

[4] T. Yoshikawa, "Dynamic manipulability of robot manipulators," in *ICRA 1985*, St. Louis, Missouri, Mar. 1985, pp. 1033–1038.

[5] ——, *Foundations of Robotics: Analysis and Control*. The MIT Press, 1990.

[6] H. Kim, L. Miller, and J. Rosen, "Redundancy resolution of a human arm for controlling a seven dof wearable robotic system," in *EMBC 2011*, Boston, USA, Aug. 2011.

[7] J. Soechting, C. Buneo, U. Herrmann, and M. Flanders, "Moving effortlessly in three dimensions: does donders' law apply to arm movement?" *J. Neuroscience*, vol. 15, no. 9, pp. 6271–6280, 1995.

[8] T. Kang, J. He, and S. I. H. Tillery, "Determining natural arm configuration along a reaching trajectory," *Exp Brain Res*, vol. 167, pp. 352–361, 2005.

[9] N. Hogan, "An organizing principle for a class of voluntary movements," *J. of Neuroscience*, vol. 4, no. 2, pp. 2745–2754, 1984.

[10] T. Flash and N. Hogan, "The coordination of arm movements: an experimentally confirmed mathematical model," *J. of Neurophysiology*, vol. 5, pp. 1688–1703, 1985.

[11] Y. Uno, M. Kawato, and R. Suzuki, "Formation and control of optimal trajectory in human multijoint arm movement - minimum torque-change model," *Biology Cybernetics*, vol. 61, pp. 89–101, 1989.

[12] E. Nakano, H. Imamizu, R. Osu, Y. Uno, H. Gomi, T. Yoshioka, and M. Kawato, "Quantitative examinations of internal representations for arm trajectory planning: Minimum commanded torque change model," *The Journal of Neurophysiology*, vol. 81, no. 5, pp. 2140–2155, 1999.

[13] C. M. Harris and D. M. Wolpert, "Signal-dependent noise determines motor planning," *Nature*, vol. 194, pp. 780–784, 1998.

[14] E. Todorov and M. I. Jordan, "Optimal feedback control as a theory of motor coordination," *Nature Neuroscience*, vol. 5, pp. 1226–1235, 2002.

[15] N. I. Badler and D. Tolani, "Real-time inverse kinematics of the human arm," *Presence*, vol. 5, no. 4, pp. 393–401, 1996.

[16] I. A. Kapandji, L. Honore, and R. Tubiana, *Physiology of the Joints*. Elsevier - Health Sciences Division, 2007.

[17] F. E. Mount, M. Whitmore, and S. L. Stealey, "Evaluation of neutral body posture on shuttle mission sts-57 (spacehab-1)," Tech. Rep., Feb 2003.

[18] W. H. DuMouchel and F. L. O'Brien, "Integrating a robust option into a multiple regression computing environment." in *Computer Science and Statistics: Proc. 21st Symposium on the Interface*, Alexandria, VA, pp. 41–48.